frontiers in Energy Research

ORIGINAL RESEARCH
published: 14 March 2022
doi: 10.3389/fenrg.2022.871617

One-step Synthesis of Biomass-Based Carbon Dots for Detection of Metal Ions and Cell Imaging

Xiaolin Huang[1†], Jiaheng Liu[1†], Bin Zhao[1], Yibing Bai[1], Zhibin Peng[2], Jundan Zhou[1], Chenxi Wang[1], Xuan Zhao[1], Shiyan Han[1] and Chunlei Zhang[1]**

[1]Key Laboratory of Bio-Based Material Science and Technology (Northeast Forestry University), Ministry of Education, Harbin, China, [2]Department of Orthopedic Surgery, The First Affiliated Hospital of Harbin Medical University, Harbin, China

Biomass-based carbon dots (Bio-CDs) were prepared from dehydroabietic acid using a one-step hydrothermal process. Characterization by TEM, XPS and FTIR spectroscopy showed that the Bio-CDs are spherical nanoparticles containing mainly C, N and O elements, with functional groups such as amino and carbonyl groups on their surface. The optical properties of the Bio-CDs were studied in detail. A solution of Bio-CDs exhibited excitation-dependent blue fluorescence emission. The solution showed excellent photostability under ultraviolet light and the fluorescence intensity could be enhanced by decreasing the temperature. The intensity of fluorescence emission of the solution was essentially unchanged over the pH range 3.91–8.69, and in the presence of different anions and cations, other than Fe^{3+} and Pb^{2+}. Fe^{3+} and Pb^{2+} ions, respectively, quenched and enhanced the intensity of the fluorescence emission of the solution, allowing sensitive and selective detection of Fe^{3+} (LOD = 2.33 μM, Em = 437 nm) and of Pb^{2+} (LOD = 0.27 μM, Em = 437 nm and LOD = 0.33 μM, Em = 500 nm). As a further demonstration of potential applications, the Bio-CDs were shown to have low cytotoxicity and to stain cell nuclei as effectively as the commonly used nuclear stain 4′,6-diamino-2-phenylindole (DAPI), demonstrating their promise in the field of cell imaging.

Keywords: dehydroabietic acid, carbon dots, detection of Fe3+, detection of Pb2+, cell imaging

OPEN ACCESS

Edited by:
Shuangxi Nie,
Guangxi University, China

Reviewed by:
Jiang Guiquan,
Beihua University, China
Hua Ma,
Massachusetts General Hospital and Harvard Medical School, United States

****Correspondence:***
Shiyan Han
hanshiyan80@163.com
Chunlei Zhang
zhangchunlei@nefu.edu.cn

[†]These authors have contributed equally to this work

Specialty section:
This article was submitted to Electrochemical Energy Conversion and Storage, a section of the journal Frontiers in Energy Research

Received: *08 February 2022*
Accepted: *21 February 2022*
Published: *14 March 2022*

Citation:
Huang X, Liu J, Zhao B, Bai Y, Peng Z, Zhou J, Wang C, Zhao X, Han S and Zhang C (2022) One-step Synthesis of Biomass-Based Carbon Dots for Detection of Metal Ions and Cell Imaging. Front. Energy Res. 10:871617. doi: 10.3389/fenrg.2022.871617

INTRODUCTION

With increasing global realization of the importance of sustainable resources and energy, forest-based biomass resources and the development of highly processed products have become areas of intense research interest (Klemm et al., 2005; Yao et al., 2013; Yu et al., 2014; Liu et al., 2021d; Liu et al., 2021f). Many highly processed products derived from biomass resources, including cellulose, lignin, and rosin and its derivatives, have been widely studied (Li et al., 2016; Li et al., 2019b; Liu et al., 2020; Song et al., 2020; Liu et al., 2021e; Nie et al., 2021). Such products have been developed for use in energy storage (Sun et al., 2014; Liu et al., 2021b; Liu et al., 2021c; Xu et al., 2021), catalysis (An et al., 2019; Li et al., 2021c), sensing (Du et al., 2019a; Zhang et al., 2021a; Miao et al., 2021; Yuan et al., 2021; Zhao et al., 2021; Liu et al., 2022) and biomedicine (Du et al., 2019a; Liu et al., 2020), etc. Biomass resources have gradually become one of the main sources of photoluminescent chemicals because they are abundant, inexpensive, easy availability and have good sustainability (Ge et al., 2021a; Cai et al., 2021; Wareing et al., 2021; Yu et al., 2021). Photoluminescent materials derived from biomass resources include fluorescent organic molecules (He et al., 2018; Han et al., 2020) and carbon dots (Ge et al., 2021b; Ge et al., 2021c; Li et al., 2021b; Tan et al., 2021); the latter have been widely

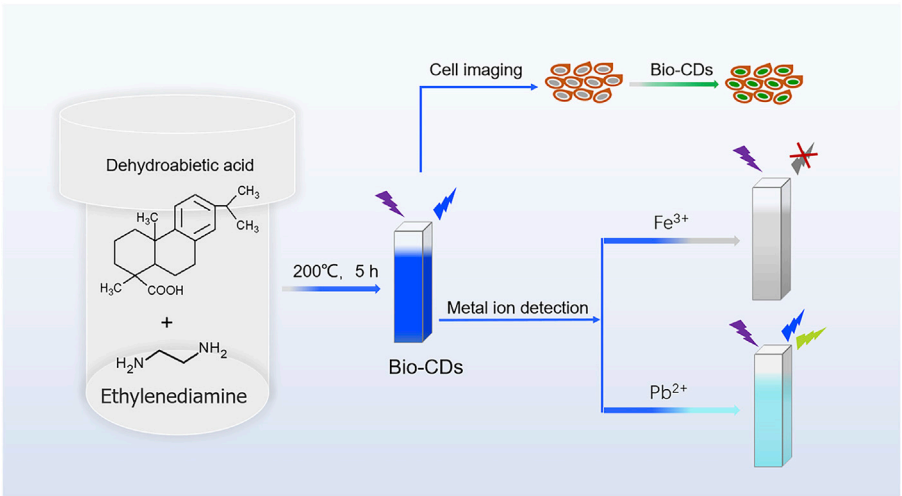

SCHEME 1 | Formation of biomass-based carbon dots for detection of metal ions and cell imaging.

studied because they are non-toxic, have good biocompatibility and optical tunability and also demonstrate strong photoluminescence (Su et al., 2020; Wang et al., 2021a; Zhang et al., 2021b). Carbon dots are discrete quasi-spherical nanoparticles, with particle sizes of less than 10 nm (Li et al., 2021a), the surfaces of which can be decorated with various functional groups, such as –NH2, –C=O, –OH and –COOH (Du et al., 2019b; Li et al., 2021a). Because of their favorable physical, chemical and biomedical properties, such as broad absorption spectra, tunable fluorescence, and excellent photostability and biocompatibility, carbon dots have been widely used as functional optical materials in fluorescence sensing, bioimaging and other fields (Liu et al., 2019; Li et al., 2020; Khairol Anuar et al., 2021; Li et al., 2021d; Wang et al., 2021b).

With the acceleration of urbanization and industrialization, environmental pollution is becoming an increasingly serious global problem. Heavy metal ions, which are not biodegradable, are considered to be the most toxic pollutants (Zhao et al., 2019) and pollution of water with heavy metal ions is one of the most serious environmental problems in the world (Bolisetty et al., 2016; Ko et al., 2017). The ability to detect trace amounts of heavy metal ions in water with high sensitivity and specificity is critical for waste management, environmental protection and water safety. Conventional techniques for detecting and analyzing metal ions often require expensive instrumentation and/or complex sample preparation, such as emission spectroscopy or atomic absorption, anodic stripping voltammetry, inductively coupled plasma mass spectrometry and capillary electrophoresis. Thus, it is urgent to explore new sensing technologies that can detect metal ions with simpler operation, higher sensitivity and selectivity and lower costs. With the development of nanoscale science and engineering, fluorescence nanoprobes are currently the most commonly used analytical tools for detecting metal ions because of their high sensitivity, selectivity, efficiency and low costs. (Zhang et al., 2016; Li et al., 2020). We now describe a one-step hydrothermal synthesis of water-soluble biomass-based carbon dots (Bio-CDs) from dehydroabietic acid and ethylenediamine. The Bio-CDs can be used as fluorescent probes to detect Fe^{3+} with limits of detection (LOD) of 2.33 μM (Em = 437 nm); Pb^{2+} with LODs of 0.27 μM (Em = 437 nm) and 0.33 μM (Em = 500 nm), respectively. The Bio-CDs can also be used for cell imaging, with the same nuclear imaging capability as commercially available 4′,6-diamino-2-phenylindole (DAPI) (**Scheme 1**).

MATERIALS AND METHODS

Materials

Dehydroabietic acid (99.06%) was purchased from Jusheng Technology Co., Ltd. (Hubei, China). Ethylenediamine, $Al(NO_3)_3{\cdot}9H_2O$, $NaH_2PO_2{\cdot}H_2O$, $Ca(NO_3)_2{\cdot}4H_2O$,$Cd(NO_3)_2{\cdot}4H_2O$, $Cu(NO_3)_2{\cdot}3H_2O$, $Fe(NO_3)_3{\cdot}9H_2O$, $AgNO_3$ and $NaNO_3$ were purchased from Bodi Chemical Industry Co., Ltd. (Tianjin, China). $Ni(NO_3)_2{\cdot}6H_2O$, $Pb(NO_3)_2$, $Sr(NO_3)_2$, $Ba(NO_3)_2$, $C_2H_2ClO_2Na$, CH_3COONa and $NaNO_2$ were purchased from Fuyu Fine Chemical Co., Ltd. (Tianjin, China). EDTA-2Na, $B_4O_7Na_2$, $C_2O_4Na_2$, Na_2HPO_4, NaCl, NaF, $NaHCO_3$, $Co(NO_3)_2{\cdot}6H_2O$, $FeCl_2$, Na_2SO_3, Na_2SO_4, Na_2SiO_3, $Na_2S_2O_3$ and NaH_2PO_4 were purchased from Yongda Chemical Reagent Co., Ltd. (Tianjin, China). All chemicals were of analytical purity and were used as received. Deionized water was prepared using a smart-q30 UT ultrapure water system (Zhiang Instrument Co., Ltd., Shanghai, China). The cell counting kit-8 (CCK-8) assay was purchased from Dojindo Laboratories (Kumamoto, Japan), Normocin was purchased from InvivoGen (San Diego, CA, United States). Dulbecco's modified Eagle's medium/Ham's F12 medium (DMEM/F12), phosphate-buffered saline (PBS), and fetal bovine serum (FBS) were all Gibco brand and were purchased from Thermo Fisher Scientific Inc., Waltham, MA, United States). HUVECs was purchased from the Chinese Academy of Sciences (Shanghai, China).

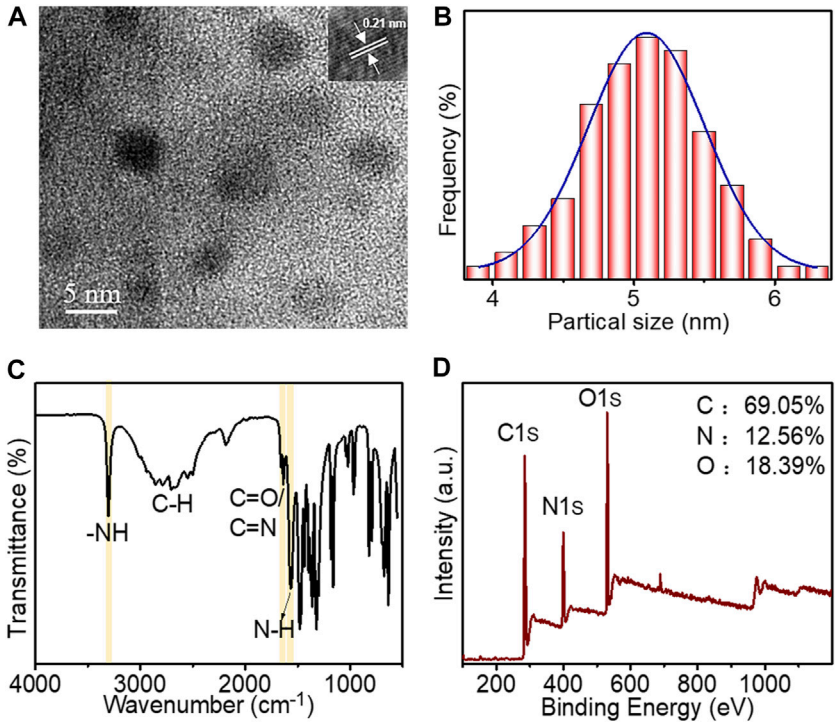

FIGURE 1 | (A) TEM image of Bio-CDs (inset: high resolution TEM image of Bio-CDs); **(B)** Particle size distribution of Bio-CDs; **(C)** FT-IR spectrum of Bio-CDs; **(D)** Full XPS spectrum of Bio-CDs.

Characterization

The morphology, structure and atomic composition of the Bio-CDs were determined using a JEM-2100 transmission electron microscope (JEOL Ltd., Tokyo, Japan), a Fourier Transform infrared (FTIR) spectrometer (Perkin Elmer Inc., Waltham, MA, United States) and an ESCALAB 250Xi X-ray photoelectron spectrometer (Thermo Fisher Scientific, New York, NY, United States), respectively. The ultraviolet-visible (UV-vis) absorption spectrum was recorded using a TU-1950 spectrofluorometer (Persee General Instrument Co., Ltd., Beijing, China). Fluorescence was measured using an LS55 fluorescence spectrometer (Perkin Elmer Inc., Waltham, MA, United States). Time-resolved fluorescence spectra were recorded using a DeltaFlex modular fluorescence lifetime instrument (Horiba Jobin Yvon IBH, Ltd., Glasgow, United Kingdom). Fluorescence images were captured using a DMI4000 B inverted fluorescence microscope (Leica Microsystems Inc., Wetzlar, Germany).

Synthesis of Bio-CDs

Ethylenediamine (1 ml) was added to a mixture of dehydroabietic acid (0.4 g) and deionized water (60 ml) in a 100 ml Teflon-lined stainless autoclave and the mixture was stirred thoroughly using a glass rod. The mixture was heated to 200°C for 5 h and then allowed to cool to room temperature. The resulting solution was filtered through a 0.22 μm ultrafiltration membrane and then freeze-dried to provide the crude product. The crude product was ground to a powder, dissolved it with absolute ethanol, and filtered to separate insoluble matter. The insoluble matter was dried under vacuum at 50°C to provide Bio-CDs.

RESULTS AND DISCUSSION

Characterization of Bio-CDs

Transmission electron microscopy (TEM) showed that the Bio-CDs were nanoparticles (**Figure 1A**), with a particle size distribution of 3.9–6.3 nm and an average diameter of 5.07 nm (**Figure 1B**). The lattice fringe spacing of the Bio-CDs, observed in high-resolution TEM (HRTEM) images, was 0.21 nm (**Figure 1A**, inset), which corresponds to the graphene (100) plane (Chen et al., 2016; Zheng et al., 2021). The FT-IR spectrum (**Figure 1C**) of the Bio-CDs showed an absorption peak at 3,305 cm^{-1}, which is characteristic of -NH stretching vibrations (Li et al., 2019a; Shi et al., 2017). The absorption peaks at 1,665 cm^{-1} and 1,637 cm^{-1} correspond to the stretching vibration of C=O/C=N groups (Chen et al., 2017; Miao et al., 2018; Shi et al., 2017). A strong peak at 1,566 cm^{-1} was attributed to N−H bending vibrations (Guo et al., 2019; Shi et al., 2017; Zhu et al., 2013). The FT-IR spectrum thus confirmed the presence of functional groups such as amino and carbonyl groups on the surface of the Bio-CDs. The full X-ray photoelectron spectroscopy (XPS) spectrum (**Figure 1D**) showed peaks at 285 eV, 399.8 and 530.9 eV, corresponding to C 1s (69.05%), N 1s (12.56%) and O 1s (18.39%), respectively. The high-resolution C 1s spectrum showed a peak at 284.5 eV,

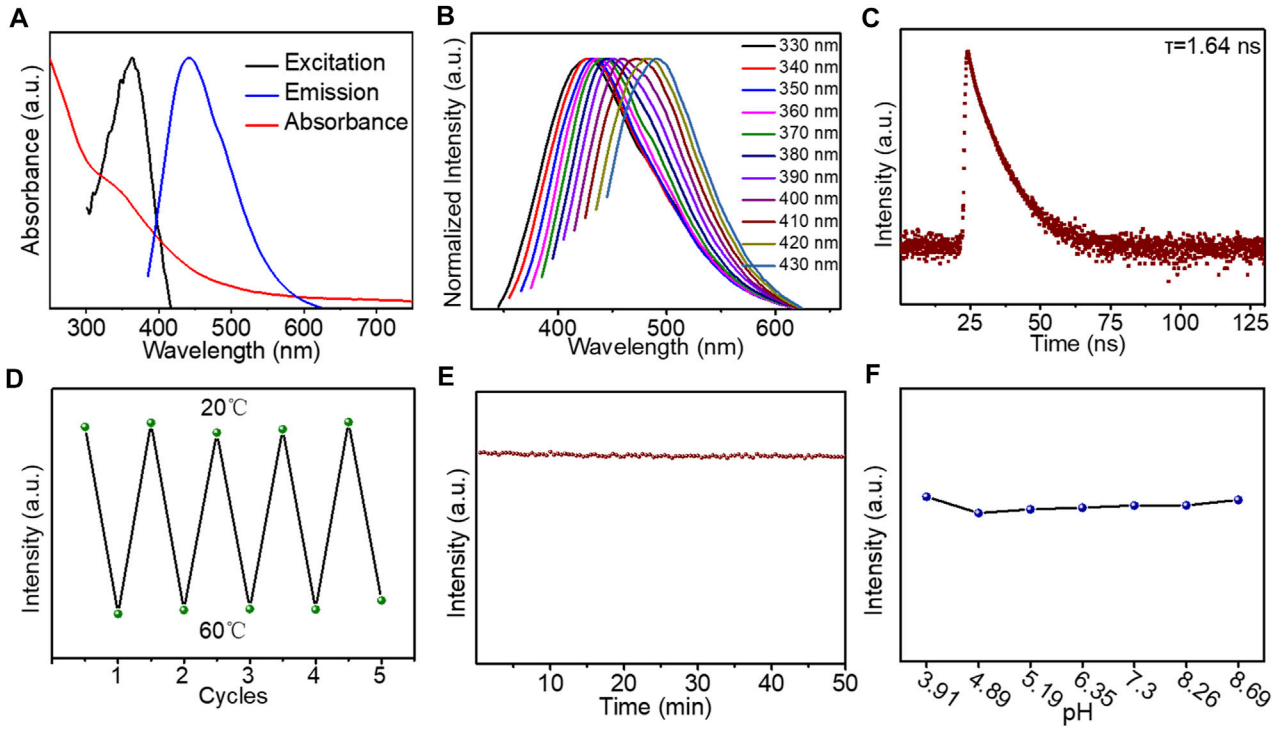

FIGURE 2 | (A) Absorption, excitation and emission spectra of aqueous solution of Bio-CDs; **(B)** Normalized fluorescence intensity of aqueous solution of Bio-CDs at different excitation wavelengths; **(C)** Time-resolved fluorescence spectrum of Bio-CDs; **(D)** Changes in fluorescence intensity of aqueous solution of Bio-CDs on repeated cycling between 20 and 70°C; **(E)** Intensity of fluorescence emission of aqueous solution of Bio-CDs (1 mg ml^{-1}) excited at 365 nm for 50 min; **(F)** Changes in fluorescence intensity of aqueous solutions of Bio-CDs at different pH values.

attributed to C–C/C=C (Bi et al., 2018; Li et al., 2019a), a peak at 285.8 eV, attributed to C–O/C–N (Nie et al., 2014; Lee et al., 2021) and a peak at 288.2 eV, attributed to C=O/C=N (Bi et al., 2018; Li et al., 2019a) (**Supplementary Figure S1A**). The high-resolution O1s spectrum showed two components, corresponding to O=C (530.9 eV) (Miao et al., 2018) and C–OH/C–O–C (532.3 eV) (Nie et al., 2014), repectively (**Supplementary Figure S1B**). The high-resolution N 1s spectrum showed peaks at 399.2 and 400.9 eV (**Supplementary Figure S1C**), corresponding to amino N (Jiao et al., 2020; Ge et al., 2021b) and pyrrole N (Sheng et al., 2011; Chen et al., 2017), respectively. All of these results indicate that the Bio-CDs have a large number of functional groups. The rich surface functionalization means that the Bio-CDs are highly soluble in water, which is very important for practical applications.

Optical Properties of Bio-CDs

Having established the physical characteristics of the Bio-CDs, we next systematically investigated their optical properties, including UV-vis absorption, photoluminescence (PL) excitation, PL emission, PL decay and PL stability (**Figure 2**). The UV absorption spectrum of an aqueous solution of Bio-CDs showed a strong absorption peak at ~300 nm and a shoulder peak at 345 nm (**Figure 2A**), which were attributed to π-π* transitions of C=C and n-π* transitions of C=O/C=N bonds, respectively (Jiang et al., 2020; Jiao et al., 2020; Wei et al., 2020). In the PL spectrum of an aqueous solution of Bio-CDs (**Figure 2B**), the emission wavelength gradually shifted from 427 to 491 nm as the excitation wavelength was increased from 330 to 430 nm. An aqueous solution of Bio-CDs thus show excitation-dependent emission, which is common among previously reported Bio-CDs (Ge et al., 2021c; Zhou et al., 2020). The optimal excitation wavelength of an aqueous solution of Bio-CDs is 370 nm and the maximum emission wavelength is 442 nm; both the optimal excitation and maximum emission wavelengths of solutions of Bio-CDs are essentially unaffected by changes in the concentration of the solution (**Supplementary Figure S2**). The PL excitation spectrum of an aqueous solution of Bio-CDs is consistent with the PL emission spectrum (**Figure 2A**). The excitation spectrum coincides with the UV absorption at 345 nm (**Figure 2A**), indicating that the emission of an aqueous solution of Bio-CDs is associated with the surface state (Liu et al., 2021a). The time-resolved fluorescence spectrum of an aqueous solution of Bio-CDs (**Figure 2C**) shows that the average fluorescence lifetime is 1.64 ns, fitted by the double exponential decay function. We also recorded the change in fluorescence intensity of an aqueous solution of Bio-CDs (λ_{ex} = 370 nm) at different temperatures. The emission intensity weakened with increasing temperature (**Figure 2D** and **Supplementary Figure S3**), and the fluorescence intensity remained essentially unchanged over several temperature

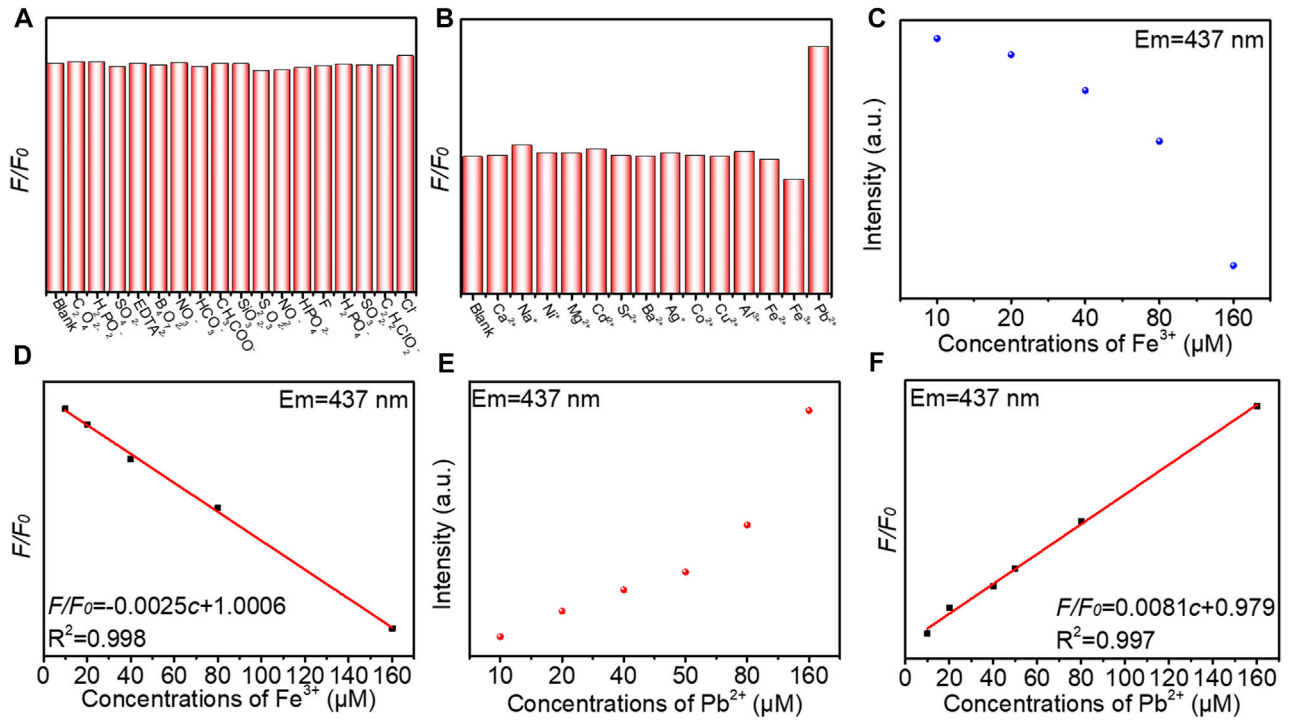

FIGURE 3 | (A,B) Fluorescence intensity ratio (F/F_0) of aqueous solution of Bio-CDs (20 μg ml^{-1}) on addition of different ions, where F and F_0 are the fluorescence intensities with and without ions, respectively; **(C)** Changes in fluorescence intensity of aqueous solution of Bio-CDs (20 μg ml^{-1}) in the presence of different concentrations of Fe^{3+}; **(D)** Dependence of F_0/F on the concentration of Fe^{3+} ions over the range 10–160 μM; **(E)** Changes in fluorescence intensity of aqueous solution of Bio-CDs (20 μg/ml) in the presence of different concentrations of Pb^{2+}; **(F)** Dependence of F_0/F on concentration of Pb^{2+} ions over the range 10–160 μM.

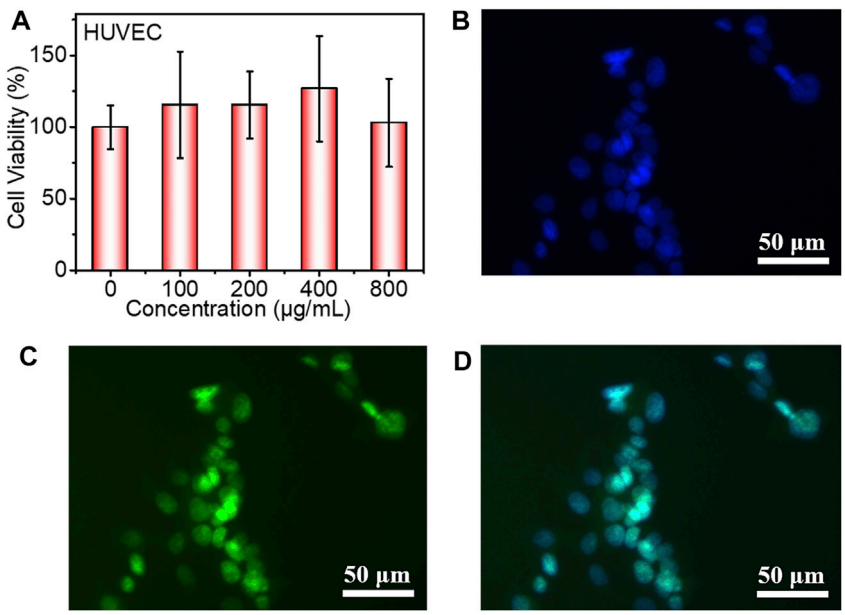

FIGURE 4 | (A) Cell viability of HUVECs incubated with different concentrations of Bio-CDs for 24 h; **(B)** Image showing nuclear staining of HUVECs by DAPI; **(C)** Image showing nuclear staining of HUVECs by Bio-CDs; **(D)** Overlay of images shown in **(B)** and **(C)**.

cycles (**Supplementary Figure S4**). The phenomenon of decreasing emission intensity with increasing temperature is associated with non-radiative relaxation (Ge et al., 2021b; Nie et al., 2014). The fluorescence intensity did not change when an aqueous solution of Bio-CDs was continuously excited with 365 nm UV light for 50 min (**Figure 2E**). The emission intensity of an aqueous solution of Bio-CDs was also essentially unchanged when the pH of the solution was adjusted between 3.91 and 8.69 (**Figure 2F** and **Supplementary Figure S5**). This is the pH range of the intracellular microenvironment, indicating that the Bio-CDs are suitable for cell imaging (Cosnier et al., 2014).

Selectivity and Sensitivity of Bio-CDs for Different Ions

Over recent years, carbon dots have been widely studied for use as ion probes (Li et al., 2020; Liu et al., 2019; Zhou et al., 2020). The fluorescence response of Bio-CDs to various anions and cations was measured by adding the test ion (50 μM) to an aqueous solution of Bio-CDs (20 μg ml^{-1}) and measuring the fluorescence intensity of the solution before (F_0) and after (F) addition of the test ion. Anions had no effect on the fluorescence intensity of the solution of Bio-CDs (**Figure 3A**). Among the tested cations, Fe^{3+} ions significantly quenched the fluorescence intensity and Pb^{2+} ions significantly enhanced the fluorescence intensity of Bio-CDs **(Figure 3B)**, whereas the other cations had no effect. The selective quenching of the fluorescence of Bio-CDs by Fe^{3+} ions is attributable to coordination of the Fe^{3+} ions with amino groups on the surface of the Bio-CDs, which disrupts radiative transition and leads to quenching of fluorescence (Atchudan et al., 2018; Gao et al., 2019). We next explored the feasibility of using Bio-CDs to detect Fe^{3+}. The fluorescence intensity of the Bio-CDs decreased significantly on addition of Fe^{3+} ions (**Figure 3C** and **Supplementary Figure S6**) and, over the range 0–160 μM, the ratio of Fe^{3+} concentration to fluorescence intensity (F_0/F) fitted well to the linear equation $F/F_0 = -0.0025c + 1.0006$, where c is the concentration of Fe^{3+} (**Figure 3D**). The LOD was 2.33 μM, based on a signal-to-noise ratio of 3 (3σ/m, where σ is the standard deviation of the blank signal (over three tests) and m is the slope of the linear fit). Because lead is a soft metal, it can covalently or synergistically interact with N-containing groups, such as the many amino groups on the surface of the Bio-CDs, which provide high affinity binding sites for Pb^{2+} ions. A large number of amino groups on the surface of the Bio-CDs can coordinate with Pb^{2+}, thus enhancing the fluorescence intensity of the Bio-CDs (Li et al., 2020). We next explored the feasibility of using Bio-CDs to detect Pb^{2+} ions (Li et al., 2020). The intensity of the fluorescence emission of the Bio-CDs (at 437 and 500 nm) was significantly enhanced by the addition of Pb^{2+} (**Figure 3E**, **Supplementary Figure S7** and **Supplementary Figure S8A**), with the emission intensity at 437 nm increasing significantly faster than that at 500 nm (**Supplementary Figure S7**). Over the range 0–160 μM, the emission intensity of Bio-CDs at 437 and 500 nm and the ratio of Pb^{2+} concentration to fluorescence intensity (F_0/F) fitted well to the linear equations $F/F_0 = 0.0081c + 0.979$ and $F/F_0 = 0.0134c + 1.0624$, respectively (**Figure 3F** and **Supplementary Figure S8B**). The LOD values were 0.27 and 0.33 μM, respectively, showing that the Bio-CDs are well suited to the detection of trace amounts of Pb^{2+}.

Cytotoxicity of Bio-CDs and Use for Cell Imaging

It has been widely reported that Bio-CDs can be used for cell imaging (Atchudan et al., 2016; Demir et al., 2018; Khairol Anuar et al., 2021; Wang et al., 2021b). Here, we used a standard cell counting kit-8 (CCK-8) to determine the cytotoxicity of Bio-CDs in HUVECs (Zhou et al., 2020). Bio-CDs were found to have good biocompatibility and not to show cytotoxicity when incubated with HUVECs for 24 h, at concentrations as high as 800 μg ml^{-1} (**Figure 4A**). We next investigated the potential of Bio-CDs for cell imaging by incubating them with HUVECs for 10 h (Zhou et al., 2020). Cells stained with DAPI, a commonly used nuclear stain, and with Bio-CDs are shown in **Figure 4B** and **Figure 4C**, respectively. The two images overlap well (**Figure 4D**), demonstrating that Bio-CDs can also be used as an effective nuclear stain.

CONCLUSION

Bio-CDs were prepared from dehydroabietic acid and ethylenediamine, using a one-step hydrothermal reaction. An aqueous solution of Bio-CDs emitted blue fluorescence when irradiated with a 365 nm UV lamp and the Bio-CDs showed good stability, resistance to photobleaching and biocompatibility. As examples of practical applications, when used as a fluorescent probe, the LOD for Fe^{3+} ions was 2.33 μM (Em = 437 nm) and those for Pb^{2+} were 0.27 μM (Em = 437 nm) and 0.33 μM (Em = 500 nm). When used for cell imaging, stained the nucleus of HUVECs just as effectively as the commercially available nuclear stain, DAPI. It is proved that the Bio-CDs can be used both for sensitive and selective detection of heavy metal ions and for whole cell imaging.

DATA AVAILABILITY STATEMENT

The original contributions presented in the study are included in the article/**Supplementary Material**, further inquiries can be directed to the corresponding authors.

AUTHOR CONTRIBUTIONS

XH and JL conducted experiments and analyses. XH wrote the first draft of the manuscript. ZP conducted cell imaging

experiments. SH and CZ put forward the research idea, obtained funds, supervised the writing of manuscripts and carried out revisions. The other authors made substantial, direct and intellectual contributions to the work. All authors approved the final version of the manuscript.

FUNDING

These authors contributed equally to this work. This work was supported by the National Natural Science Foundation of China (32171715), the Hei Long Jiang Postdoctoral Foundation (LBH-Q21003) and the National Undergraduate Training Program for Innovation (202110225167). The authors are grateful for the funding.

SUPPLEMENTARY MATERIAL

The Supplementary Material for this article can be found online at: https://www.frontiersin.org/articles/10.3389/fenrg.2022.871617/full#supplementary-material

REFERENCES

An, L. L., Si, C. L., Wang, G. H., Sui, H. J., and Tao, Z. Y. (2019). Enhancing the Solubility and Antioxidant Activity of High-Molecular-Weight Lignin by Moderate Depolymerization via *In Situ* Ethanol/acid Catalysis. *Ind. Crops Prod.* 128, 177–185. doi:10.1016/j.indcrop.2018.11.009

Atchudan, R., Edison, T. N. J. I., and Lee, Y. R. (2016). Nitrogen-doped Carbon Dots Originating from Unripe Peach for Fluorescent Bioimaging and Electrocatalytic Oxygen Reduction Reaction. *J. Colloid Interf. Sci.* 482, 8–18. doi:10.1016/j.jcis.2016.07.058

Atchudan, R., Edison, T. N. J. I., Aseer, K. R., Perumal, S., Karthik, N., and Lee, Y. R. (2018). Highly Fluorescent Nitrogen-Doped Carbon Dots Derived from Phyllanthus Acidus Utilized as a Fluorescent Probe for Label-free Selective Detection of Fe3+ Ions, Live Cell Imaging and Fluorescent Ink. *Biosens. Bioelectron.* 99, 303–311. doi:10.1016/j.bios.2017.07.076

Bi, Z. H., Li, T. W., Su, H., Ni, Y., and Yan, L. F. (2018). Transparent Wood Film Incorporating Carbon Dots as Encapsulating Material for White Light-Emitting Diodes. *ACS Sust. Chem. Eng.* 6, 9314–9323. doi:10.1021/acssuschemeng.8b01618

Bolisetty, S., and Mezzenga, R. (2016). Amyloid-carbon Hybrid Membranes for Universal Water Purification. *Nat. Nanotech* 11, 365–371. doi:10.1038/nnano.2015.310

Cai, X. M., Lin, Y. T., Li, Y., Chen, X. F., Wang, Z. Y., Zhao, X. Q., et al. (2021). BioAIEgens Derived from Rosin: How Does Molecular Motion Affect Their Photophysical Processes in Solid State? *Nat. Commun.* 12, 1773. doi:10.1038/s41467-021-22061-y

Chen, Y. H., Zheng, M. T., Xiao, Y., Dong, H. W., Zhang, H. R., Zhuang, J. L., et al. (2016). A Self-Quenching-Resistant Carbon-Dot Powder with Tunable Solid-State Fluorescence and Construction of Dual-Fluorescence Morphologies for White Light-Emission. *Adv. Mater.* 28, 312–318. doi:10.1002/adma.201503380

Chen, J., Wei, J. S., Zhang, P., Niu, X. Q., Zhao, W., Zhu, Z. Y., et al. (2017). Red-Emissive Carbon Dots for Fingerprints Detection by Spray Method: Coffee Ring Effect and Unquenched Fluorescence in Drying Process. *ACS Appl. Mater. Inter.* 9, 18429–18433. doi:10.1021/acsami.7b03917

Cosnier, S., Le Goff, A., and Holzinger, M. (2014). Towards Glucose Biofuel Cells Implanted in Human Body for Powering Artificial Organs: Review. *Electrochemistry Commun.* 38, 19–23. doi:10.1016/j.elecom.2013.09.021

Demir, B., Lemberger, M. M., Panagiotopoulou, M., Medina Rangel, P. X., Timur, S., Hirsch, T., et al. (2018). Tracking Hyaluronan: Molecularly Imprinted Polymer Coated Carbon Dots for Cancer Cell Targeting and Imaging. *ACS Appl. Mater. Inter.* 10, 3305–3313. doi:10.1021/acsami.7b16225

Du, H. S., Liu, W. M., Zhang, M. L., Si, C. L., Zhang, X. Y., and Li, B. (2019a). Cellulose Nanocrystals and Cellulose Nanofibrils Based Hydrogels for Biomedical Applications. *Carbohydr. Polym.* 209, 130–144. doi:10.1016/j.carbpol.2019.01.020

Du, J. J., Xu, N., Fan, J. L., Sun, W., and Peng, X. (2019b). Carbon Dots for *In Vivo* Bioimaging and Theranostics. *Small* 15, 1805087. doi:10.1002/smll.201805087

Gao, X. X., Zhou, X., Ma, Y. F., Qian, T., Wang, C. P., and Chu, F. X. (2019). Facile and Cost-Effective Preparation of Carbon Quantum Dots for Fe^{3+} Ion and Ascorbic Acid Detection in Living Cells Based on the "On-Off-On" Fluorescence Principle. *Appl. Surf. Sci.* 469, 911–916. doi:10.1016/j.apsusc.2018.11.095

Ge, M., Han, S. Y., Ma, Y. L., Li, J., Liu, S. X., Chen, Z. J., et al. (2021a). Sensitive Mechanofluorochromic Carbon Dot-Based AIEgens: Promising Reporting Components for Self-Sensing Plastics. *Adv. Opt. Mater.* 9, 2101092. doi:10.1002/adom.202101092

Ge, M., Han, Y. Q., Ni, J. X., Li, Y. D., Han, S. Y., Li, S. J., et al. (2021b). Seeking Brightness from Nature: Sustainable Carbon Dots-Based AIEgens with Tunable Emission Wavelength from Natural Rosin. *Chem. Eng. J.* 413, 127457. doi:10.1016/j.cej.2020.127457

Ge, M., Huang, X., Ni, J. X., Han, Y. Q., Zhang, C. L., Li, S. J., et al. (2021c). One-step Synthesis of Self-Quenching-Resistant Biomass-Based Solid-State Fluorescent Carbon Dots with High Yield for white Lighting Emitting Diodes. *Dyes Pigm.* 185, 108953. doi:10.1016/j.dyepig.2020.108953

Guo, X., Xu, D., Yuan, H. M., Luo, Q. Y., Tang, S. Y., Liu, L., et al. (2019). A Novel Fluorescent Nanocellulosic Hydrogel Based on Carbon Dots for Efficient Adsorption and Sensitive Sensing in Heavy Metals. *J. Mater. Chem. A.* 7, 27081–27088. doi:10.1039/c9ta11502a

Han, S. Y., Ni, J. X., Han, Y. Q., Ge, M., Zhang, C. L., Jiang, G. Q., et al. (2020). Biomass-Based Polymer Nanoparticles with Aggregation-Induced Fluorescence Emission for Cell Imaging and Detection of Fe3+ Ions. *Front. Chem.* 8, 563. doi:10.3389/fchem.2020.00563

He, T., Niu, N., Chen, Z. J., Li, S. J., Liu, S. X., and Li, J. (2018). Novel Quercetin Aggregation-Induced Emission Luminogen (AIEgen) with Excited-State Intramolecular Proton Transfer for *In Vivo* Bioimaging. *Adv. Funct. Mater.* 28, 1706196. doi:10.1002/adfm.201706196

Jiang, K., Gao, X. L., Feng, X. Y., Wang, Y. H., Li, Z. J., and Lin, H. W. (2020). Carbon Dots with Dual-Emissive, Robust, and Aggregation-Induced Room-Temperature Phosphorescence Characteristics. *Angew. Chem. Intl Edit* 59, 1263–1269. doi:10.1002/anie.201911342

Jiao, Y., Liu, Y., Meng, Y. T., Gao, Y. F., Lu, W. J., Liu, Y., et al. (2020). Novel Processing for Color-Tunable Luminescence Carbon Dots and Their Advantages in Biological Systems. *ACS Sust. Chem. Eng.* 8, 8585–8592. doi:10.1021/acssuschemeng.0c01016

Khairol Anuar, N. K., Tan, H. L., Lim, Y. P., So'aib, M. S., and Abu Bakar, N. F. (2021). A Review on Multifunctional Carbon-Dots Synthesized from Biomass Waste: Design/Fabrication, Characterization and Applications. *Front. Energ. Res.* 9, 626549. doi:10.3389/fenrg.2021.626549

Klemm, D., Heublein, B., Fink, H.-P., and Bohn, A. (2005). Cellulose: Fascinating Biopolymer and Sustainable Raw Material. *Angew. Chem. Int. Ed.* 44, 3358–3393. doi:10.1002/anie.200460587

Ko, D., Lee, J. S., Patel, H. A., Jakobsen, M. H., Hwang, Y., Yavuz, C. T., et al. (2017). Selective Removal of Heavy Metal Ions by Disulfide Linked Polymer Networks. *J. Hazard. Mater.* 332, 140–148. doi:10.1016/j.jhazmat.2017.03.007

Lee, U., Heo, E., Le, T.-H., Lee, H., Kim, S., Lee, S., et al. (2021). Carbon Dots for Epoxy Curing: Anti-forgery Patterns with Long-Term Luminescent Stability. *Chem. Eng. J.* 405, 126988. doi:10.1016/j.cej.2020.126988

Li, Y. N., Liu, Y. Z., Chen, W. S., Wang, Q. W., Liu, Y. X., Li, J., et al. (2016). Facile Extraction of Cellulose Nanocrystals from wood Using Ethanol and Peroxide Solvothermal Pretreatment Followed by Ultrasonic Nanofibrillation. *Green. Chem.* 18, 1010–1018. doi:10.1039/c5gc02576a

Li, W. T., Hu, X. T., Li, Q., Shi, Y. Q., Zhai, X. D., Xu, Y. W., et al. (2020). Copper Nanoclusters @ Nitrogen-Doped Carbon Quantum Dots-Based Ratiometric Fluorescence Probe for lead (II) Ions Detection in Porphyra. *Food Chem.* 320, 126623. doi:10.1016/j.foodchem.2020.126623

Li, W., Zhou, W., Zhou, Z. S., Zhang, H. R., Zhang, X. J., Zhuang, J. L., et al. (2019a). A Universal Strategy for Activating the Multicolor Room-Temperature Afterglow of Carbon Dots in a Boric Acid Matrix. *Angew. Chem. Int. Ed.* 58, 7278–7283. doi:10.1002/anie.201814629

Li, X., Xu, R., Yang, J. X., Nie, S. X., Liu, D., Liu, Y., et al. (2019b). Production of 5-hydroxymethylfurfural and Levulinic Acid from Lignocellulosic Biomass and Catalytic Upgradation. *Ind. Crops Prod.* 130, 184–197. doi:10.1016/j.indcrop.2018.12.082

Li, W., Chen, Z. J., Yu, H. P., Li, J., and Liu, S. X. (2021c). Wood-Derived Carbon Materials and Light-Emitting Materials. *Adv. Mater.* 33, 2000596. doi:10.1002/adma.202000596

Li, X., Lu, S. Y., Mu, X. J., Li, T. R., Sun, S. H., Zhao, Y., et al. (2021d). Red-light-responsive Coordination Polymers Nanorods: New Strategy for Ultrasensitive Photothermal Detection of Targeted Cancer Cells. *Biosens. Bioelectron.* 190, 113417. doi:10.1016/j.bios.2021.113417

Li, B. L., Zhao, S. J., Huang, L., Wang, Q., Xiao, J. F., and Lan, M. H. (2021a). Recent Advances and Prospects of Carbon Dots in Phototherapy. *Chem. Eng. J.* 408, 127245. doi:10.1016/j.cej.2020.127245

Li, D., Ushakova, E. V., Rogach, A. L., and Qu, S. N. (2021b). Optical Properties of Carbon Dots in the Deep-Red to Near-Infrared Region Are Attractive for Biomedical Applications. *Small* 17, 2102325. doi:10.1002/smll.202102325

Liu, F., Li, Z. Y., Li, Y., Feng, Y. Y., and Feng, W. (2021a). Room-temperature Phosphorescent Fluorine-Nitrogen Co-doped Carbon Dots: Information Encryption and Anti-counterfeiting. *Carbon* 181, 9–15. doi:10.1016/j.carbon.2021.05.023

Liu, H. Y., Du, H., Zheng, T., Liu, K., Ji, X., Xu, T., et al. (2021b). Cellulose Based Composite Foams and Aerogels for Advanced Energy Storage Devices. *Chem. Eng. J.* 426, 130817. doi:10.1016/j.cej.2021.130817

Liu, H. Y., Xu, T., Liu, K., Zhang, M., Liu, W., Li, H., et al. (2021c). Lignin-based Electrodes for Energy Storage Application. *Ind. Crops Prod.* 165, 113425. doi:10.1016/j.indcrop.2021.113425

Liu, K., Du, H., Liu, W., Liu, H., Zhang, M., Xu, T., et al. (2021d). Cellulose Nanomaterials for Oil Exploration Applications. *Polym. Rev.*, 1–41. doi:10.1080/15583724.2021.2007121

Liu, K., Du, H. S., Zheng, T., Liu, H. Y., Zhang, M., Zhang, R., et al. (2021e). Recent Advances in Cellulose and its Derivatives for Oilfield Applications. *Carbohydr. Polym.* 259, 117740. doi:10.1016/j.carbpol.2021.117740

Liu, K., Du, H. S., Zheng, T., Liu, W., Zhang, M., Liu, H., et al. (2021f). Lignin-containing Cellulose Nanomaterials: Preparation and Applications. *Green. Chem.* 23, 9723–9746. doi:10.1039/D1GC02841C

Liu, Z. Y., Jin, W. Y., Wang, F. X., Li, T. C., Nie, J. F., Xiao, W. C., et al. (2019). Ratiometric Fluorescent Sensing of Pb2+ and Hg2+ with Two Types of Carbon Dot Nanohybrids Synthesized from the Same Biomass. *Sensors Actuators B: Chem.* 296, 126698. doi:10.1016/j.snb.2019.126698

Liu, W., Du, H. S., Zhang, M. M., Liu, K., Liu, H. Y., Xie, H. X., et al. (2020). Bacterial Cellulose-Based Composite Scaffolds for Biomedical Applications: A Review. *ACS Sust. Chem. Eng.* 8, 7536–7562. doi:10.1021/acssuschemeng.0c00125

Liu, H., Xu, T., Cai, C., Liu, K., Liu, W., Zhang, M., et al. (2022). Multifunctional Superelastic, Superhydrophilic, and Ultralight Nanocellulose-Based Composite Carbon Aerogels for Compressive Supercapacitor and Strain Sensor. *Adv. Funct. Mater.* 32, 2113082. doi:10.1002/adfm.202113082

Miao, S., and Cho, Y. (2021). Toward Green Optoelectronics: Environmental-Friendly Colloidal Quantum Dots Photodetectors. *Front. Energ. Res.* 9, 666534. doi:10.3389/fenrg.2021.666534

Miao, X., Qu, D., Yang, D. X., Nie, B., Zhao, Y. K., Fan, H. Y., et al. (2018). Synthesis of Carbon Dots with Multiple Color Emission by Controlled Graphitization and Surface Functionalization. *Adv. Mater.* 30, 1704740. doi:10.1002/adma.201704740

Nie, H., Li, M. J., Li, Q. S., Liang, S. J., Tan, Y. Y., Sheng, L., et al. (2014). Carbon Dots with Continuously Tunable Full-Color Emission and Their Application in Ratiometric pH Sensing. *Chem. Mater.* 26, 3104–3112. doi:10.1021/cm5003669

Nie, S. X., Fu, Q., Lin, X. J., Zhang, C. Y., Lu, Y. X., and Wang, S. F. (2021). Enhanced Performance of a Cellulose Nanofibrils-Based Triboelectric Nanogenerator by Tuning the Surface Polarizability and Hydrophobicity. *Chem. Eng. J.* 404, 126512. doi:10.1016/j.cej.2020.126512

Sheng, Z.-H., Shao, L., Chen, J.-J., Bao, W.-J., Wang, F.-B., Xia, X.-H., et al. (2011). Catalyst-Free Synthesis of Nitrogen-Doped Graphene via Thermal Annealing Graphite Oxide with Melamine and its Excellent Electrocatalysis. *ACS Nano* 5, 4350–4358. doi:10.1021/nn103584t

Shi, R., Li, Z., Yu, H. J., Shang, L., Zhou, C., Waterhouse, G. I. N., et al. (2017). Effect of Nitrogen Doping Level on the Performance of N-Doped Carbon Quantum Dot/TiO2 Composites for Photocatalytic Hydrogen Evolution. *ChemSusChem* 10, 4650–4656. doi:10.1002/cssc.201700943

Song, J. X., Wu, Y., Ma, X. J., Feng, L. J., Wang, Z. G., Jiang, G. Q., et al. (2020). Structural Characterization and α-glycosidase Inhibitory Activity of a Novel Polysaccharide Fraction from Aconitum Coreanum. *Carbohydr. Polym.* 230, 115586. doi:10.1016/j.carbpol.2019.115586

Su, Y., Xie, Z. G., and Zheng, M. (2020). Carbon Dots with Concentration-Modulated Fluorescence: Aggregation-Induced Multicolor Emission. *J. Colloid Interf. Sci.* 573, 241–249. doi:10.1016/j.jcis.2020.04.004

Sun, S.-L., Wen, J.-L., Ma, M.-G., Song, X.-L., and Sun, R.-C. (2014). Integrated Biorefinery Based on Hydrothermal and Alkaline Treatments: Investigation of Sorghum Hemicelluloses. *Carbohydr. Polym.* 111, 663–669. doi:10.1016/j.carbpol.2014.04.099

Tan, J., Li, Q. J., Meng, S., Li, Y. C., Yang, J., Ye, Y. X., et al. (2021). Time-Dependent Phosphorescence Colors from Carbon Dots for Advanced Dynamic Information Encryption. *Adv. Mater.* 33, 2006781. doi:10.1002/adma.202006781

Wang, B. Y., Song, H. Q., Tang, Z. Y., Yang, B., and Lu, S. Y. (2021a). Ethanol-derived white Emissive Carbon Dots: the Formation Process Investigation and Multi-Color/white LEDs Preparation. *Nano Res.* 15, 942–949. doi:10.1007/s12274-021-3579-5

Wang, Z. X., Zhan, M. X., Li, W. J., Chu, C. Y., Xing, D., Lu, S. Y., et al. (2021b). Photoacoustic Cavitation-Ignited Reactive Oxygen Species to Amplify Peroxynitrite Burst by Photosensitization-Free Polymeric Nanocapsules. *Angew. Chem. Int. Ed.* 60, 4720–4731. doi:10.1002/anie.202013301

Wareing, T. C., Gentile, P., and Phan, A. N. (2021). Biomass-Based Carbon Dots: Current Development and Future Perspectives. *ACS Nano* 15, 15471–15501. doi:10.1021/acsnano.1c03886

Wei, J. Y., Lou, Q., Zang, J. H., Liu, Z. Y., Ye, Y. L., Shen, C. L., et al. (2020). Scalable Synthesis of Green Fluorescent Carbon Dot Powders with Unprecedented Efficiency. *Adv. Opt. Mater.* 8, 1901938. doi:10.1002/adom.201901938

Xu, T., Du, H. S., Liu, H. Y., Liu, W., Zhang, X. Y., Si, C. L., et al. (2021). Advanced Nanocellulose-Based Composites for Flexible Functional Energy Storage Devices. *Adv. Mater.* 33, 2101368. doi:10.1002/adma.202101368

Yao, K., and Tang, C. B. (2013). Controlled Polymerization of Next-Generation Renewable Monomers and beyond. *Macromolecules* 46, 1689–1712. doi:10.1021/ma3019574

Yu, J., Liu, Y. P., Liu, X. H., Wang, C. P., Wang, J. F., Chu, F. X., et al. (2014). Integration of Renewable Cellulose and Rosin towards Sustainable Copolymers by "Grafting from" ATRP. *Green. Chem.* 16, 1854–1864. doi:10.1039/c3gc41550c

Yu, J., Xu, C. Q., Lu, C. W., Liu, Q., Wang, J. F., and Chu, F. X. (2021). Synthesis of pH-Sensitive and Self-Fluorescent Polymeric Micelles Derived from Rosin and Vegetable Oils via ATRP. *Front. Bioeng. Biotechnol.* 9, 753808. doi:10.3389/fbioe.2021.753808

Yuan, Q., and Ma, M.-G. (2021). Conductive Polypyrrole Incorporated nanocellulose/MoS2 Film for Preparing Flexible Supercapacitor Electrodes. *Front. Mater. Sci.* 15, 227–240. doi:10.1007/s11706-021-0549-5

Zhang, C. Y., Mo, J. L., Fu, Q., Liu, Y. H., Wang, S. F., and Nie, S. X. (2021a). Wood-cellulose-fiber-based Functional Materials for Triboelectric Nanogenerators. *Nano Energy* 81, 105637. doi:10.1016/j.nanoen.2020.105637

Zhang, M. L., Ma, Y. R., Wang, H. B., Wang, B., Zhou, Y. J., Liu, Y., et al. (2021b). Chiral Control of Carbon Dots via Surface Modification for Tuning the Enzymatic Activity of Glucose Oxidase. *ACS Appl. Mater. Inter.* 13, 5877–5886. doi:10.1021/acsami.0c21949

Zhang, J. J., Cheng, F. F., Li, J. J., Zhu, J. J., and Lu, Y. (2016). Fluorescent Nanoprobes for Sensing and Imaging of Metal Ions: Recent Advances and

Future Perspectives. *Nano Today* 11, 309–329. doi:10.1016/j.nantod.2016.05.010

Zhao, T. Q., Zhang, K., Chen, J. W., Shi, X. B., Li, X., Ma, Y. L., et al. (2019). Changes in Heavy Metal Mobility and Availability in Contaminated Wet-Land Soil Remediated Using Lignin-Based Poly(acrylic Acid). *J. Hazard. Mater.* 368, 459–467. doi:10.1016/j.jhazmat.2019.01.061

Zhao, D. W., Zhu, Y., Cheng, W. K., Chen, W. S., Wu, Y. Q., and Yu, H. (2021). Cellulose-Based Flexible Functional Materials for Emerging Intelligent Electronics. *Adv. Mater.* 33, 2000619. doi:10.1002/adma.202000619

Zheng, Y. X., Arkin, K., Hao, J. W., Zhang, S. Y., Guan, W., Wang, L. L., et al. (2021). Multicolor Carbon Dots Prepared by Single-Factor Control of Graphitization and Surface Oxidation for High-Quality White Light-Emitting Diodes. *Adv. Opt. Mater.* 9, 2100688. doi:10.1002/adom.202100688

Zhou, J. D., Ge, M., Han, Y. Q., Ni, J. X., Huang, X., Han, S. Y., et al. (2020). Preparation of Biomass-Based Carbon Dots with Aggregation Luminescence Enhancement from Hydrogenated Rosin for Biological Imaging and Detection of Fe3+. *ACS Omega* 5, 11842–11848. doi:10.1021/acsomega.0c01527

Zhu, S. J., Meng, Q. N., Wang, L., Zhang, J. H., Song, Y. B., Jin, H., et al. (2013). Highly Photoluminescent Carbon Dots for Multicolor Patterning, Sensors, and Bioimaging. *Angew. Chem. Int. Ed.* 52, 3953–3957. doi:10.1002/anie.201300519

Conflict of Interest: The authors declare that the research was conducted in the absence of any commercial or financial relationships that could be construed as a potential conflict of interest.

Publisher's Note: All claims expressed in this article are solely those of the authors and do not necessarily represent those of their affiliated organizations, or those of the publisher, the editors and the reviewers. Any product that may be evaluated in this article, or claim that may be made by its manufacturer, is not guaranteed or endorsed by the publisher.